A New Predictive Skid Resistance Model (PSRM) for Pavement Evolution due to Texture Polishing by Traffic

Malal KANE [1)*], Michael LIM [2)], Minh Tan DO [1)], Vikki EDMONSOND [2)]

[1)] Université Gustave Eiffel, Allée des Ponts et Chaussées, 44300 Bouguenais, France.
[2)] Northumbria University, Newcastle-upon-Tyne, NE7 7YT, United Kingdom.
*Corresponding author: malal.kane@univ-eiffel.fr

Abstract

We propose a new model to predict the evolution of pavement skid resistance due to traffic polishing. The model accounts for polishing (by coupling a contact model with a wear law equation) and friction mechanisms. The contact model considers the tire operating conditions (including load, speed, and slip ratio), the tire geometry and mechanical behavior of the rubber tread, the pavement texture, and the physical properties of contaminants (i.e. the thickness and viscosity of fluids). The wear law considers the types of aggregates in the pavements (particularly their mineralogical composition) and the pressure distribution within the tire/pavement contact area. The friction component considers the mechanical behavior of a rubber measuring pad, the operating conditions during pad/pavement contact, and the pavement texture. The new predictive skid resistance evolution model is a numerical computational code that resolves pavement texture topographies at different polishing stages and the corresponding skid resistance levels. The model outcomes have been validated against repeated profilometer measurements on three mosaic pavements made of different types of aggregates subjected to the "Wehner-Schulz" procedure (that polishes and measures friction). The modeled predictions performed well against the captured changes in pavement textures during the polishing process, with slight differences in their absolute values potentially due to probable limitations of the wear law. The ability to predict the evolution of pavement skid resistance has transformative potential for tailored forecasting and proactive interventions to be undertaken across road networks.

Keywords: Roads, Skid Resistance Evolution, Texture, Polishing, Traffic, Model

Introduction

The ability of vehicle tires to grip on pavement surfaces is paramount to the safety of roads. Road grip enables vehicles to correctly follow the desired trajectories and to minimize their braking distances, especially when vehicle avoidance is required in emergency situations [1]. Surface texture is the defining parameter in the "Skid resistance" of pavements, influencing the generation of tire/pavement grip forces [2-4]. Indeed, in the tire/pavement contact area, it is the surface texture that induces several spot dissymmetrical deformations of the viscoelastic tire tread and causes the tangential forces that oppose the tire movement [4-6].

Surface texture is a combination of several sizes of irregularities, both vertically and horizontally [4, 7-11]. In studies related to skid resistance of pavements, these irregularities are often classified into two classes: microtexture and macrotexture [4, 12, 13]. The microtexture corresponds to the irregularities of dimensions ranging from 0.001 mm to 0.5 mm vertically and less than 0.5 mm horizontally [14]. These irregularities are mainly related to the roughness at the aggregate surfaces and the fine particles used in the asphalt mixes [15]. The microtexture contributes both to the generation of the hysteretic forces at the microscale level and to the breakage of the remaining water film after the thicker part has been evacuated in wet conditions. The macrotexture, on the other hand, corresponds with surface irregularities that range between 0.1 mm and 20 mm vertically and between 0.5 mm and 50 mm horizontally [14]. It is mainly controlled by the granulometric curve of the aggregates used in the asphalt mixes and the degrees of compaction during the pavement construction [16, 17]. Macrotexture contributes to the hysteretic friction at the macroscale level and also provides drainage paths for water to escape from the tire/road contact patch in wet conditions [18, 19].

The repeated polishing of surface texture by traffic results in progressive decreases in skid resistance toward a long-term limit (except in young-age pavements where skid resistance initially increases due to the stripping of the asphalt binder masking their microtexture or seasonal variations) [20, 21]. That limit or the long-term skid resistance depends mainly on the ability of the aggregates to retain their microtexture when submitted to polishing action [22-25]. This aggregate characteristic has been investigated

several times in the past [26]. The hardness of the different minerals within the aggregates has been identified as the critical determinant and recently led to the definition of an Aggregate Hardness Parameter (AHP) correlating mineral hardness with long-term skid resistance [23, 25].

Current polishing models, generally consider the material loss rate of pavements subjected to traffic as proportional to the local tire/pavement contact pressure and the aggregates' Micro Deval parameter (MDE) [27]. Despite encouraging results for mono-mineral aggregate pavements, these models give poor results when it comes to poly-mineral aggregate pavements. Indeed, MDE determines a generalized average wear resistance of the aggregates. Therefore, the AHP holds significant potential as an improved metric for texture evolution. Another limitation of current polishing models is the static aspect of their contact models. In reality, accounting for the dynamic aspects (speed and slip ratio) affecting the pressure distribution in a viscoelastic and rough contact, and consequently, the resultant material loss is essential to achieving an accurate model of the polishing process.

As for the prediction of skid resistance directly from the pavement texture, significant progress has been made recently. A robust Dynamic Friction Model (DFM) has been proposed considering several parameters related to the tire, the pavement surface, and the contact operating conditions [28, 29]. This model is capable of predicting the skid resistance of pavements from the 3D topographies of their surface textures. This model simulates the sliding of the rubber pad of the Wehner-Schulz machine (used in the present study) during the skid resistance measurement and thus forms a critical parameter for a new friction component for a new predictive skid resistance model (PSRM) proposed here.

We integrate recent advances and new process models to simulate the evolution of the skid resistance of pavements subjected to the polishing action of traffic. Using two core components, the PSRM combines polishing and friction processes. The polishing components are dedicated to reproducing the evolution of the texture during the polishing process. It improves an existing polishing model by introducing the dynamic aspects of the contact and by considering the poly-mineralogic aspects of the aggregates.

Additionally, the DFM underpins the friction component of the PSRM. To validate the PSRM, the polishing and the friction heads of the Wehner-Schulz machine are used to reproduce traffic polishing action experimentally and to measure the skid resistance on three mosaic pavements made of different aggregates. A laser profilometer captures the changes of the pavement textures at different polishing stages. The robustness of the tool is evaluated by comparing the experimental results to its predictions.

The PSRM

The model integrates two connected components below (Figure 1):

- The first accounts for the polishing process to evaluate the change in the texture. This component is composed of two different models: a contact model that calculates the pressure distribution in the dynamic tire/pavement contact, and a wear law that evaluates the material loss of the pavement surface as a function of the local contact pressure and the aggregates' AHP.
- The second component corresponds to the resultant friction. It evaluates the skid resistance provided by the texture of the pavement surface and the operating conditions of the contact.

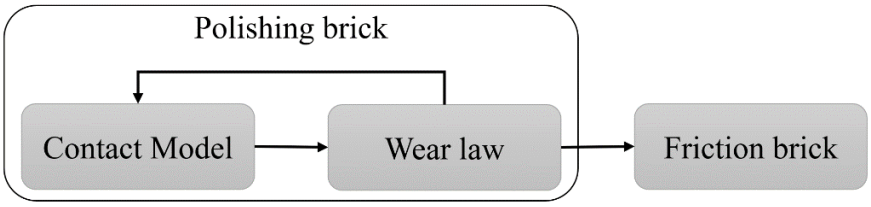

Figure 1: the model components and their interconnections of the entire model

Polishing

The pressure distribution in the tire/pavement contact area through each tire revolution needs to be coupled with a wear law in order to establish the material loss and thus the resultant change in surface texture.

Contact model

The contact model must consider the texture of the pavement surface, the geometry and mechanical characteristics of the tire (radius, width, tread grooves, tire stiffness, tread rubber viscoelasticity), the contact physics (load, speed, slip rate), and the contact

operating conditions (dry, lubricated) [30]. The tire and the pavement are introduced distinctly, with a spatial mesh corresponding to the resolution at which the texture is captured. In the governing equations (Equations 1 to 5) taken from the publication [30] and recapped here, the index i and j localize respectively a tread element and a road element (Figure 2) (See ref. 30, for further detail on the calculations).

$$\overrightarrow{F_{ij}} + \overrightarrow{T_{ij}} + \overrightarrow{R_{ij}} + \overrightarrow{FR_{ij}} = \vec{0} \qquad \text{Equation 1}$$

Where,

- $\overrightarrow{F_{ij}}$ is the local contact force applied by a tread rubber element on a surface element at a given time t. We use a "Kelvin-Voigt" model for the tire rubber, where K is the spring's stiffness per unit length and C is the dashpot's viscosity per unit length. $\overrightarrow{F_{ij}}$ is balanced by the load through the contact pressure p_{ij}. $F_{ij}(t) = l \times dx \times p_{ij}(t)$ with $p_{ij}(t) = Ku_{ij}(t) + C\frac{du_{ij}(t)}{dt}$ and $u_{ij}(t) = \delta(t) - h_i + z_j$, With, dx corresponding to the length of each of the tire tread mesh (taken equal to the capturing resolution of the pavement surface), dt is the time that a rubber element i moves from point j to j+1 of the road surface (dt = dx/V, where V is the slip speed of the element i). $u_{ij}(t)$ the displacement of the tread i^{th} element contacting j^{th} element on the road at time t. $\delta(t)$ is the solid displacement of the tire at time t. h_i represents the tire geometry. z_j is the height of the j^{th} point of the road profile.
- $\overrightarrow{T_{ij}}$ is the traction force. This force must be equal or just greater than the friction force opposing the movement.
- $\overrightarrow{R_{ij}}$ is the normal surface reaction force.
- $\overrightarrow{FR_{ij}}$ is a local friction force. $FR_{ij} = \mu_{\mathbf{loc}} R_{ij}$ when the element is moving on a "pseudo smooth inclined plan" with angle α_j. $\mu_{\mathbf{loc}}$ represents a local friction coefficient corresponding to the actual adhesion coefficient (that is nil in the wet).

The projection of Equation 1 onto axes x and z, coupled with the condition that $FR_{ij} = \mu_{loc} R_{ij}$ leads to:

$$T_{ij}(t) = F_{ij}(t)\frac{\sin(\alpha_j) + \mu_{loc}\cos(\alpha_j)}{\cos(\alpha_j) - \mu_{loc}\sin(\alpha_j)}$$ Equation 2

When a tread element is not in contact with the road surface, its contact pressure is nil, the element is subjected to a relaxation phase, and its position on the Z-axis is then determined by solving:

$$Ku_{ij}(t) + C\frac{du_{ij}(t)}{dt} = 0$$ Equation 3

At any time, t, the total load W applied by the tire on the road surface must be balanced by the normal contact pressure:

$$W = \sum_i^N F_{ij}(t)$$ Equation 4

Where N is the number of elements comprising the tire tread in the contact area. At this stage, the only unknown factors are $F_{ij}(t)$, representing the distribution of the contact forces applied by the tread to the road surface. For the calculation details, refer to the following publication [30].

The slip rate τ is introduced during the rotation of the tire via the relative positioning of the rubber and road elements at t+dt:

$$i = j + \left\lfloor \tau \times V\frac{dt}{dx} \right\rfloor$$ Equation 5

Additionally, the hydrodynamic pressure generated in the water trapped within the contact will exert an uplift force on the tread and thus decrease its penetration depth into the road asperities [30].

Figure 3 presents the workflow of the numerical calculation procedure for the contact parameters.

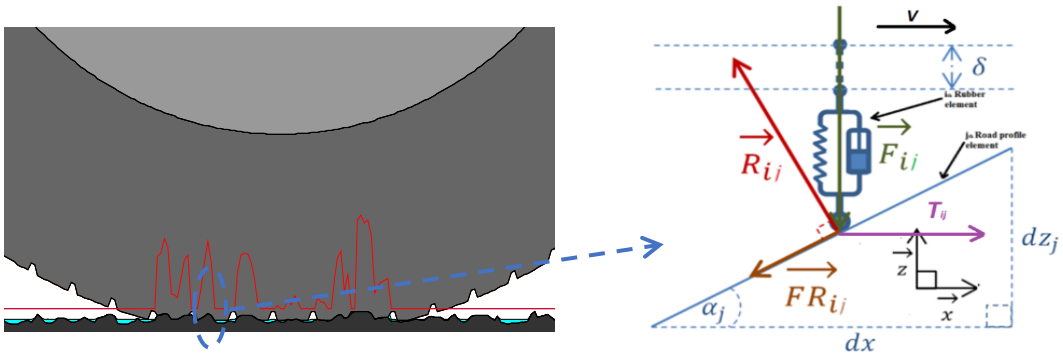

Figure 2: Forces acting between rubber and road profile elements [adapted from 30]

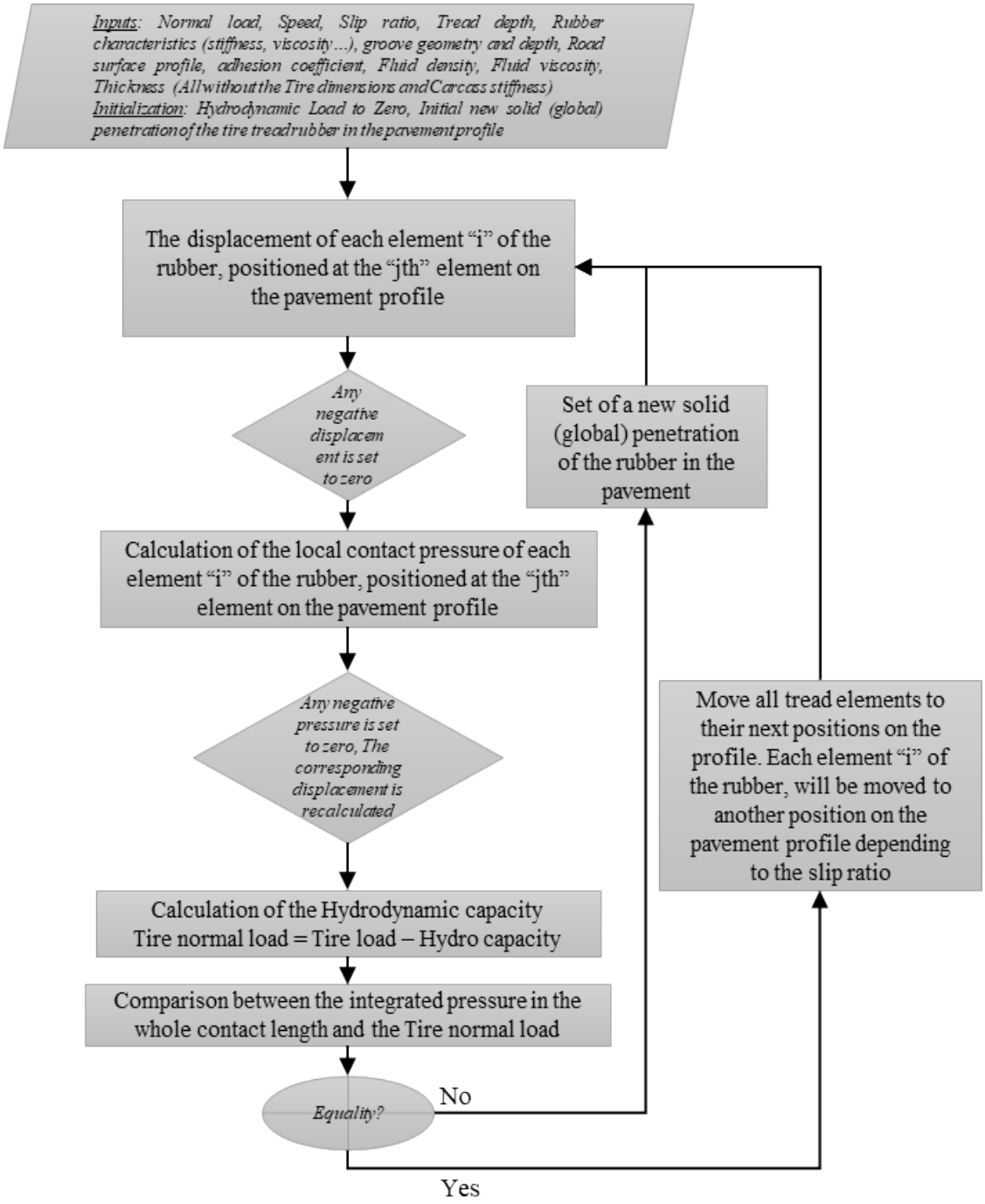

Figure 3: Numerical calculation procedure of the pressure distribution applied to the road surface by a moving tire.

Wear law

Assuming the local material removal (dz) at a given point of the pavement surface is proportional to the local contact pressure (p), the aggregates' capability to resist to wear (ACRW), and all the other constants including the operating conditions (α), the wear law

may be written as following [27] (Equation 6):

$$z_R = \frac{dz(x,y,N)}{dN} = \alpha \times ACRW \times p(x,y,N) \quad \text{Equation 6}$$

where: z_R denotes the material removal per polishing cycle, N corresponds to the number of polishing cycles, z(x,y,N) denotes the total removed material located at (x,y) after N polishing cycles and p(x,y,N) is the contact pressure at point (x,y) at the Nth cycle.

In a previous publication **Error! Reference source not found.**], the ACRW was assumed equivalent to the MDE. Here, the AHP will replace the MDE in a new wear law capable of considering the poly-mineralogy of the aggregates. Indeed, rocks with different mineral compositions can exhibit distinct behavior under the same polishing conditions. Tourenq et al. defined the "Average Hardness" and the "Contrast of Hardness" in order to explain the influence of mineralogical composition on the resistance of aggregates to polishing [26]. The polishing of a poly-mineral rock causes two phenomena: general wear, which depends on the average hardness of the rock, and differential wear, which depends on the differential contrast of hardness within the rock (Figure 4). From these two parameters, Kane et al. defined a parameter named "Aggregate Hardness Parameter" (AHP) that correlated the pavement skid resistance after long-term polishing [23, 25] (Equation 7).

$$AHP = \frac{1}{100}\sum_i H_i \times p_i + \sum_i |H_i - H_a| \quad \text{Equation 7}$$

Where: H_i is the Moh's hardness of each mineral constituting the aggregate and p_i is the percentage by mass of each mineral constituting the aggregate. H_a represents the Moh's hardness of the most abundant mineral that constitutes the aggregate.

Through these advances, the previous wear law becomes (Equation 8):

$$z_R(x,y,N,A) = \frac{\beta}{AHP} \times p(x,y,N) \quad \text{Equation 8}$$

where β is a constant including all constant parameters and is equal to 6.3 10^{-11}. The translation of calculated outcomes into reality is made with 1 cycle of polishing in the model representing 10 000 cycles of experimental polishing.

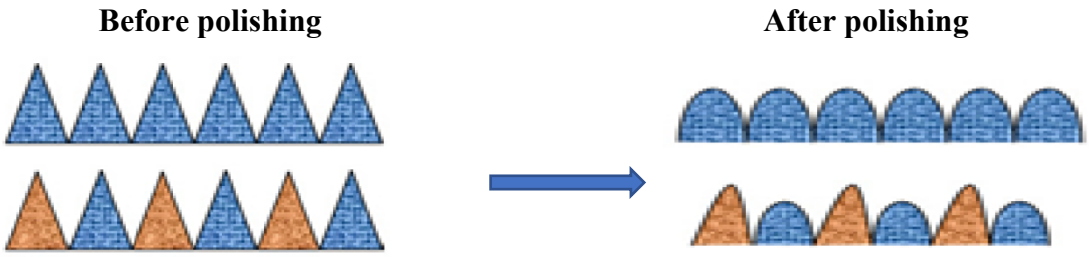

Figure 4: Illustration of the textural behavior of mono-mineral and poly-mineral aggregates during polishing.

Friction

The friction component is based on the existing DFM [28, 29]. The steps of the calculation process are similar to those of the pressure distribution calculation for the polishing component, but with two main differences relating to the contact geometry and motion. Indeed, contrary to a circular tire rolling with a slip rate on the pavement, here the moving part is a rubber pad sliding on the pavement (see Figure 5).

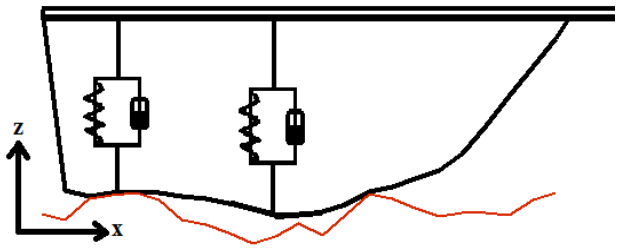

Figure 5: Geometry and mechanical model of the DFT pad

Following the same steps of the polishing contact model and the same equations (Equations 1 to 5), leading to T_{ij}, the global friction coefficient $\mu_j(t)$ can be calculated using the following formula (Equation 9):

$$\mu_j(t) = \frac{\sum_i^N T_{ij}(t)}{W} \qquad \text{Equation 9}$$

The profile of the averaged global friction coefficient μ_{av} for each pavement is calculated by averaging the friction coefficient $\mu_j(t)$ at any time iteration (Equation 10):

$$\mu_{av} = \frac{1}{M}\sum_j^M \mu_j \qquad \text{Equation 10}$$

Where M is the number of elements of the discretized pavement profile.

Application of the PSRM

Pavement specimens

It has recently been demonstrated that the skid resistance of asphalt and mosaic pavements made with the same coarse aggregates tends to the same value under long-term polishing. To avoid any effects from the asphalt components other than the aggregates, mosaics of aggregates named here "mosaic pavements" are used in this work. Three different types of aggregates, a mono-mineral (limestone) and two poly-mineral (basalt and granite) have been used to produce the pavement specimens. For each of these aggregates, a circular mosaic of 22.5 cm diameter has been prepared by placing the 7.2-10 mm size fraction of the aggregates in a single layer as closely as possible, with their flattest faces lying on the bottom of a mold and then filling the mold with a resin (Figure 8) [22].

Figure 6: Example of a pavement mosaic

A petrographic examination of each of the aggregates has been carried out. The main rock types were then identified and the relative proportions of the constituents were estimated using a microscope. Table 1 lists the mineralogical components and their hardness on the Moh's scale for the three aggregate types. The MDE of each aggregate is added for completeness [31].

Table 1: Aggregate characteristics

Aggregate type	*Mineral type (Phase)*	*Mineral Percentage*	*Mineral Hardness - Moh's scale*	**AHP**	MDE
		%	*(1 - 10)*		
Limestone	Calcite	100	3	**3,0**	12
Basalt	Pyroxene	30	5,5	**7,0**	10
	Feldspar	50	6		
	Olivine	20	6,5		
Granite	Quartz	27	7	**10,1**	9
	Feldspar	49	6		
	Amphibole	19	6		
	Biotite	5	3		

Polishing and Friction measurements

The friction measurements and the polishing of the three mosaic pavements have been performed using the two respectively dedicated heads of the Wehner-Schulze machine, a device already proven in its ability to reproduce the traffic polishing (Figure 7) [22].

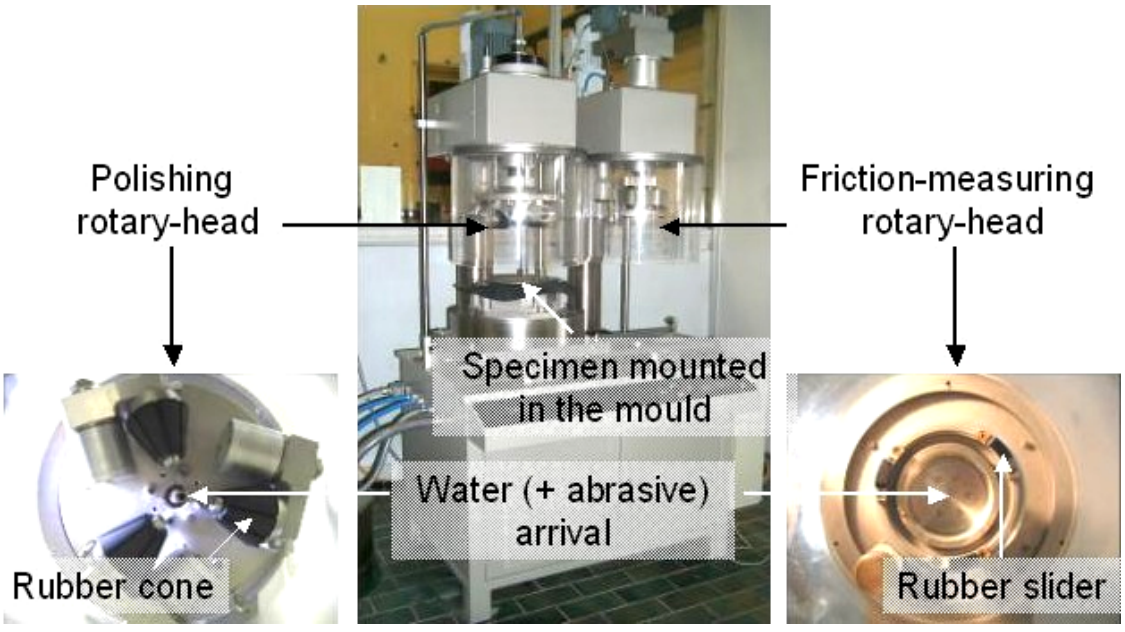

Figure 7: Wehner-Schulze machine.

The polishing head contains three rubber cones mounted on a rotary disc. It is the loaded and rolling action of these three cones on the pavement surface that produce the effect of polishing. To accelerate the polishing, a mix of 5% quartz powder in 95% water is sprinkled during the rotations of the cones. After a given number of polishing passes, the pavement is moved to the skid resistance-measuring head. This head is composed of three small rubber pads (4 cm² areas for each pad) mounted on a rotary disc. To proceed to the friction measurement, the disc is launched in up-position until a speed of 100 km/h is reached at its circumference while water is projected on the specimen surface. The motor is then stopped and the disc is dropped until the rubber pads touch the pavement surface with a contact load of approximately 0.15 N/mm². The rotation is stopped by generated friction between the rubber pads and the pavement surface. The friction–speed curve is recorded and the value at 60 km/h is used for the analyses.

Texture measurements

Texture has been captured using a laser scanning profilometer before, and after 90,000 and then 180,000 cycles of polishing (Figure 8). The measuring area is located inside the polished ring of the pavement. The topography was captured with 15 parallel profiles, 76 mm long, sampled every 0.01 mm, and separated by 0.5 mm intervals (Figure 8 - Right). Figure 9 shows the initial textures (before polishing) of the three mosaic pavements with their root mean square (Rq) and Skewness (Rsk) along the sampling length. These initial textures acted as baseline starting points for the PSRM validation procedure.

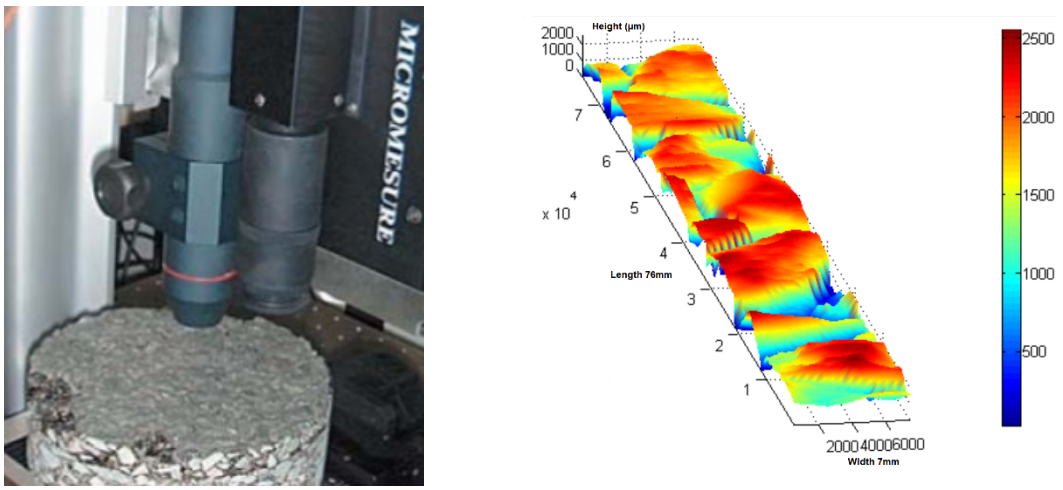

Figure 8 : Left: Profilometer, Right: Example of recorded topography

Limestone (Rsk = -0.9106, Rq = 1.7891)

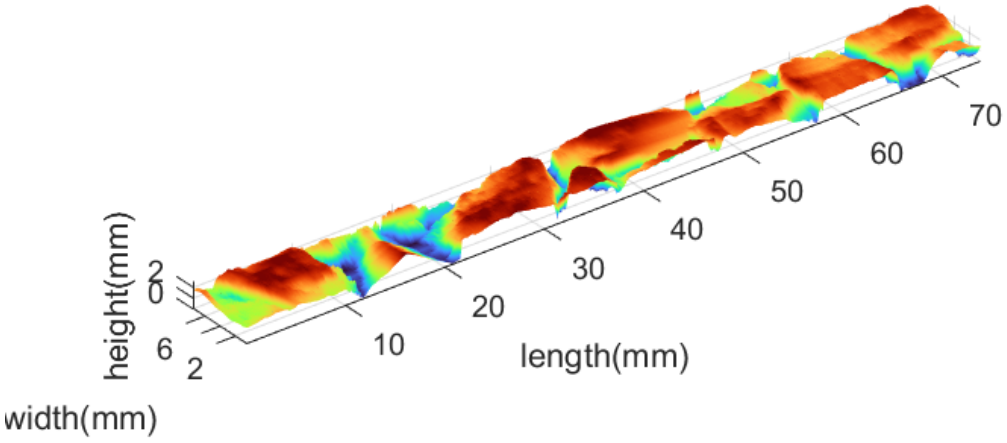

Basalt (Rsk = -1.0154, Rq = 1.9220)

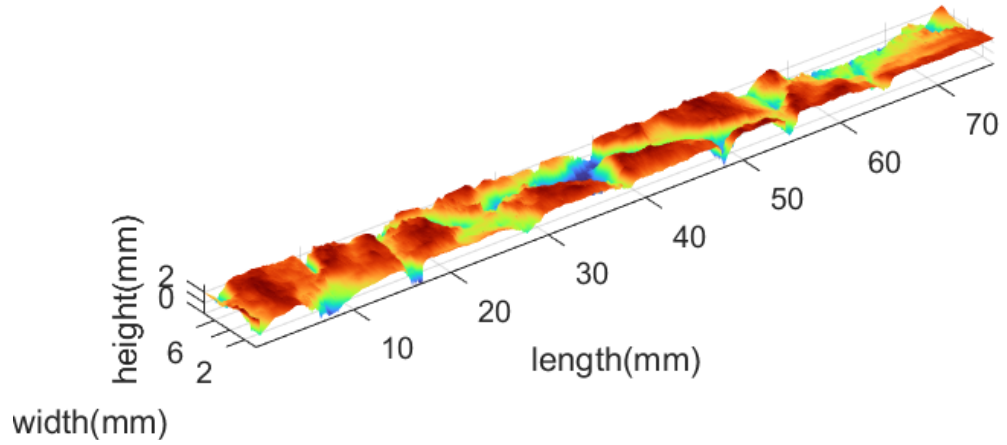

Granite (Rsk = -1.0922, Rq = 1.9252)

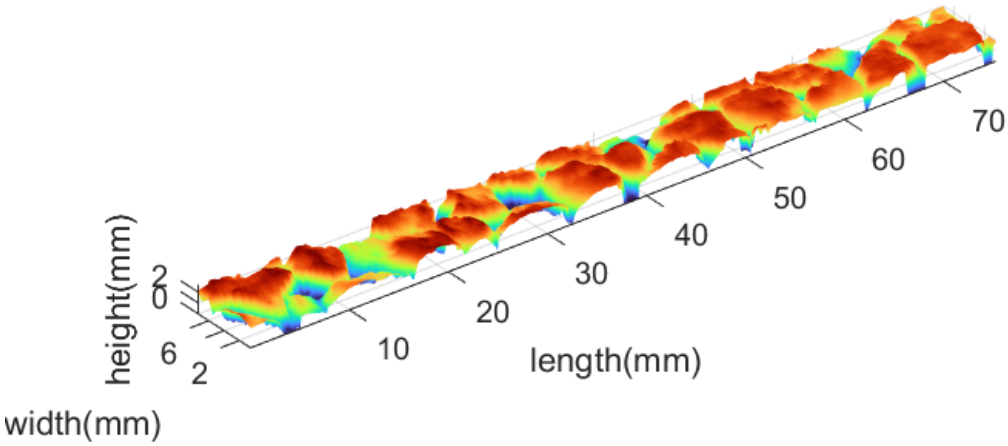

Figure 9: Initial texture topographies (before polishing) of the three mosaics recorded with the profilometer

Results and discussion

PSRM validation procedure

The predictions of the PSRM have been compared to the Wehner-Schulze skid resistance measurements at different polishing stages (after 0, 90,000, and 180,000 cycles of polishing) on the three mosaic pavement specimens of predetermined aggregate composition. The overall comparison procedure is outlined in Figure 10.

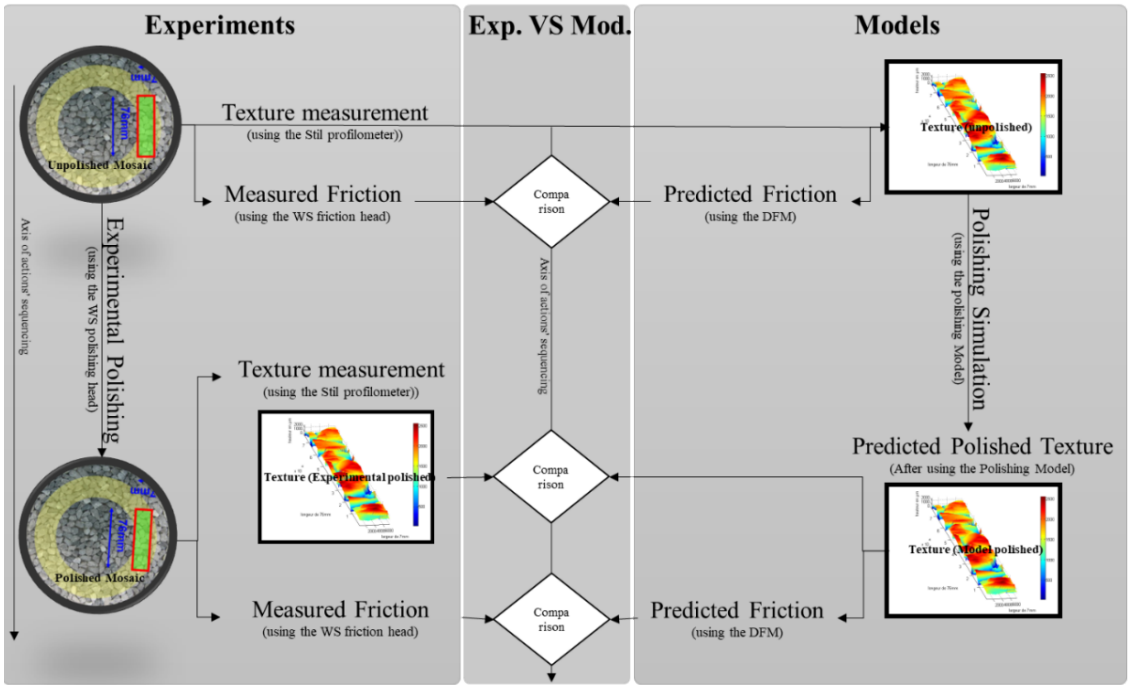

Figure 10: Illustration of the procedure to compare the PSRM predictions to the experimental results

Predicted and experimental results comparison

Table 2 displays the skid resistance values of the three mosaic pavements. The first column (named "*Pol_Exp & Fric_Exp"*) gives the skid resistance values achieved with an exclusively experimental approach, i.e. obtained after Wehner-Schulze polishing and obtaining Wehner-Schulze skid resistance measurements on the three mosaic pavements. The second column (named "*Pol_Exp & Fric_Mod"*) gives the PSRM skid resistance outputs using the DFM produced from the textures of the three mosaic pavements,

captured at set Wehner-Schulze polishing stages. For the third column (named "*Pol_Mod & Fric_Mod"*), polishing and skid resistance evaluations are done exclusively with the PSRM based upon polishing and the DFM, representing entirely modeled results.

The left-hand curve in Figure 11 is the correlation line between the first and second columns values of Table 2, while the right-hand curve is the correlation line between the results of the first and third columns. For the left-hand curve, a strong agreement is observed with an R^2 greater than 0.96. This demonstrates the robustness of the DFM for predicting the skid resistance directly from the pavement texture captured from any profilometer, as long as sufficient resolution (10 µm here) can be achieved. For the curve on the right, a strong agreement is also found, with an R^2 close to 0.94, showing only a slight reduction from the fit with the experimental data.

This lower correlation may highlight the need for an improvement of the wear law to achieve greater accuracy. The significant improvements achieved here by introducing the poly-mineral aspect of the aggregates could additionally consider their distribution and sizes. This would explain the slight underprediction of skid resistance for the granite mosaic pavement after long-term polishing.

Table 2: Experimental and PSRM's values of the three mosaic pavements at different polishing stages

		Pol_Exp & Fric_Exp	*Pol_Exp & Fric_Mod*	*Pol_Mod & Fric_Mod*
Limestone	*Initial*	0,440	0,440	0,440
	90K	0,208	0,233	0,255
	180K	0,195	0,212	0,201
Basalt	*Initial*	0,455	0,423	0,423
	90K	0,282	0,299	0,307
	180K	0,253	0,261	0,268
Granite	*Initial*	0,555	0,548	0,548
	90K	0,462	0,421	0,442
	180K	0,425	0,400	0,380

This observation is further evident in the individual analysis of skid resistance curves for each mosaic pavement (Figure 12). The blue circles represent the exclusively experimental Wehner-Schulze results (column 1 "*Pol_Exp & Fric_Exp*" of Table 2), the red squares represent the values obtained by running the DFM on the textures captured

by the profilometer at different Wehner-Schulze polishing stages of the mosaic pavements (column 2 "*Pol_Exp & Fric_Mod*" of Table 2), the grey triangles correspond to the exclusive PSRM outcomes (column 3 "*Pol_Mod & Fric_Mod*" of Table 2).

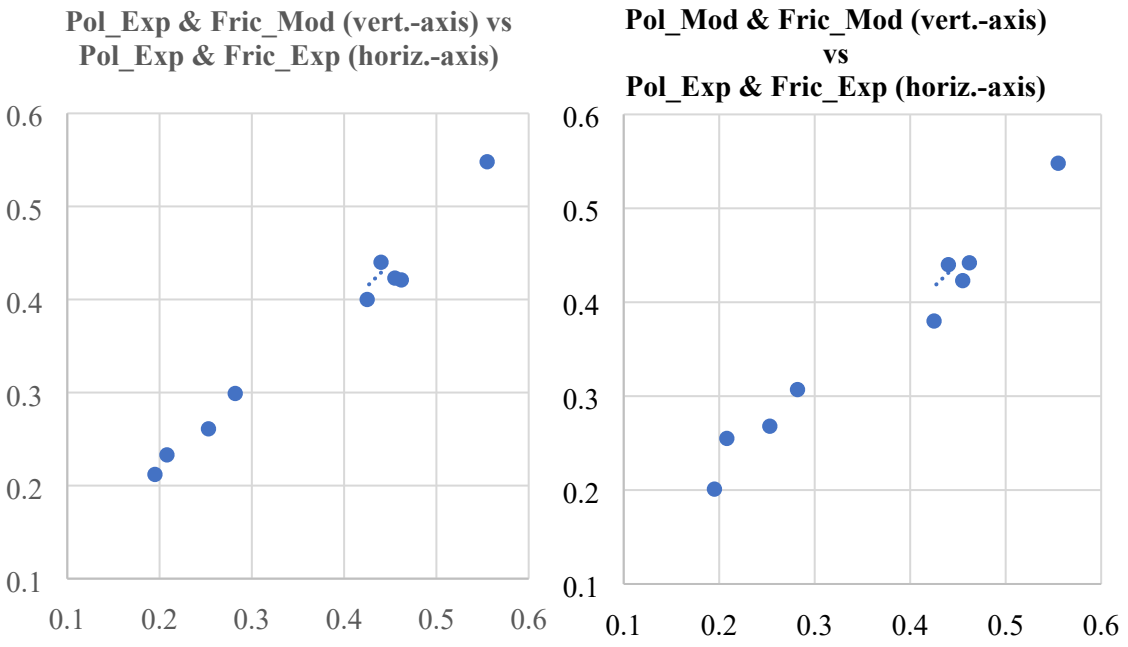

Figure 11: The left-hand curve compares the results of the first and second columns in Table 2, while the right-hand curve compares the results of the first and third columns.

When analyzing the roughness parameters, the Rq of the texture captured after Wehner-Schulze polishing for Limestone and Basalt pavements increases, which goes against the loss of material induced by polishing (Figure 9 et Figure 13). These contradictory results highlight the critical need to keep an absolute reference when trying to repeatedly measure the texture at the same location at different polishing stages.

However, despite these possible further improvements, the PSRM and its ability to consider traffic and pavement conditions have already demonstrated significant potential for a range of applications. For example, it explains why pavements situated at braking zones display lower skid resistance (e.g. highway exit ramps) or why a poly-mineral aggregate is less sensitive to the effect of traffic than a mono-mineral aggregate.

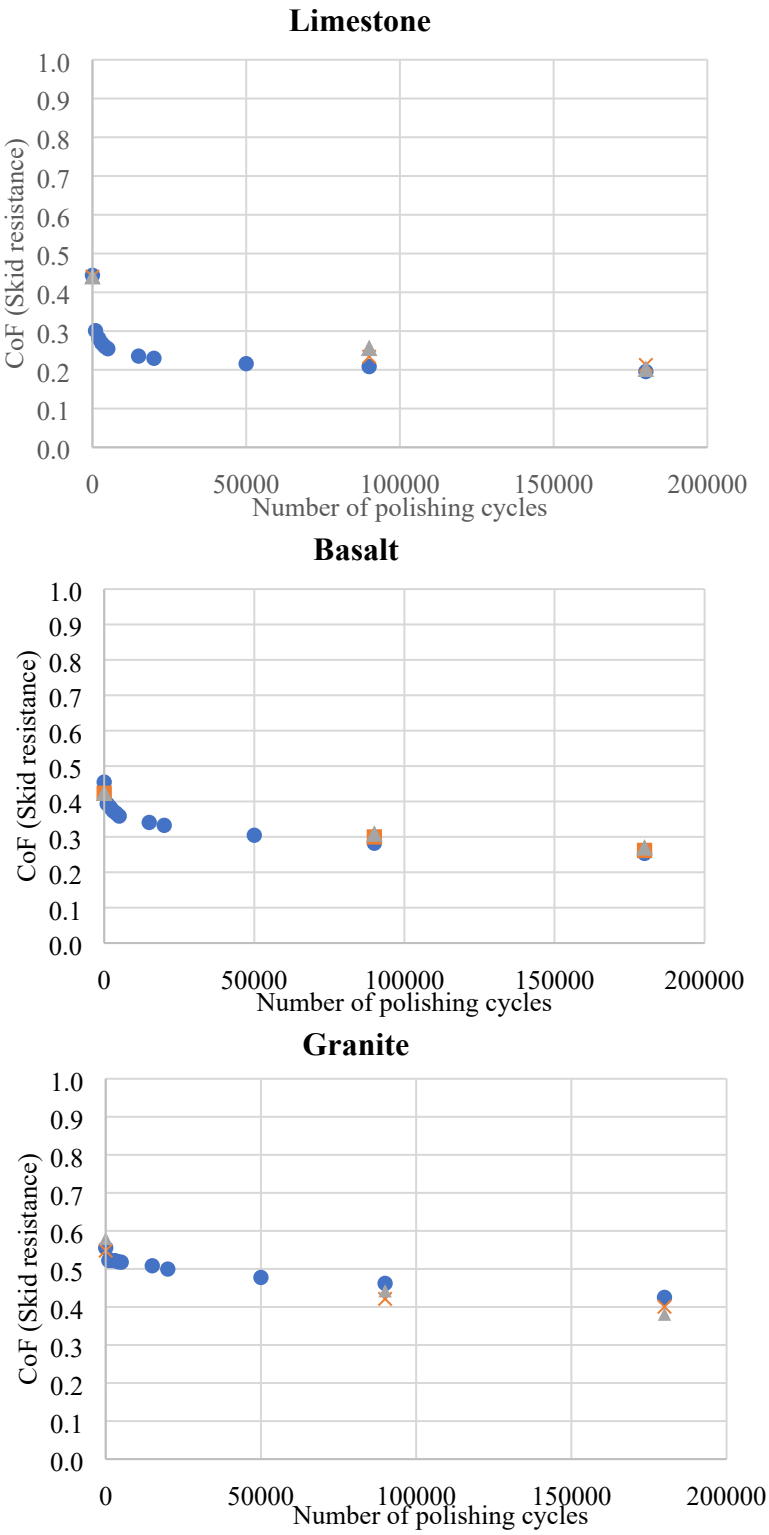

Figure 12: Comparison between the PSRM predictions and the experimental results: skid resistance evolution curves of each mosaic pavement separately (The blue circles represent the exclusively experimental Wehner-Schulze results, the red squares represent the values obtained by running the DFM on the textures captured by the profilometer at different Wehner-Schulze polishing stages of the mosaic pavements, the grey triangles correspond to the exclusive PSRM outcomes)

Limestone

Final experimental texture
(Rsk = -1.4889, Rq = 1.8716)

Final model texture
(Rsk = -1.0140, Rq = 1.7401)

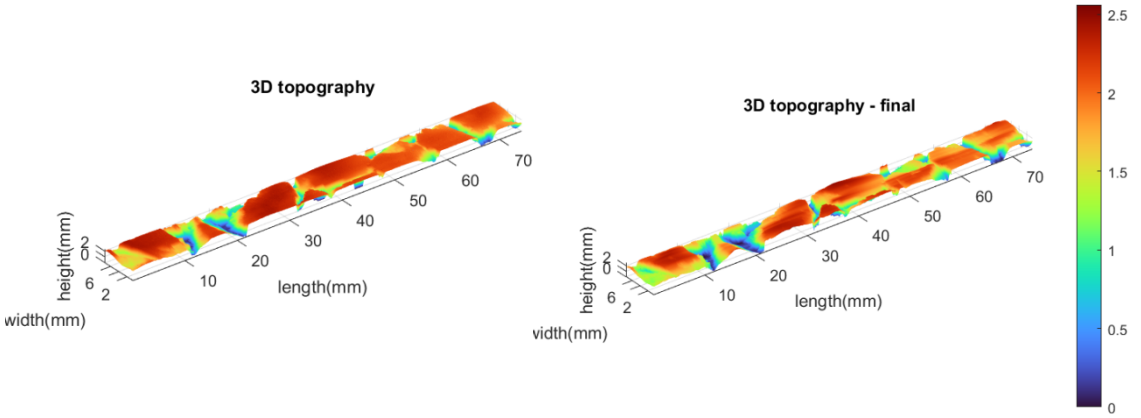

Basalt

Final experimental texture
(Rsk = -1.3104, Rq = 2.1396)

Final model texture
(Rsk = -1.0908, Rq = 1.901

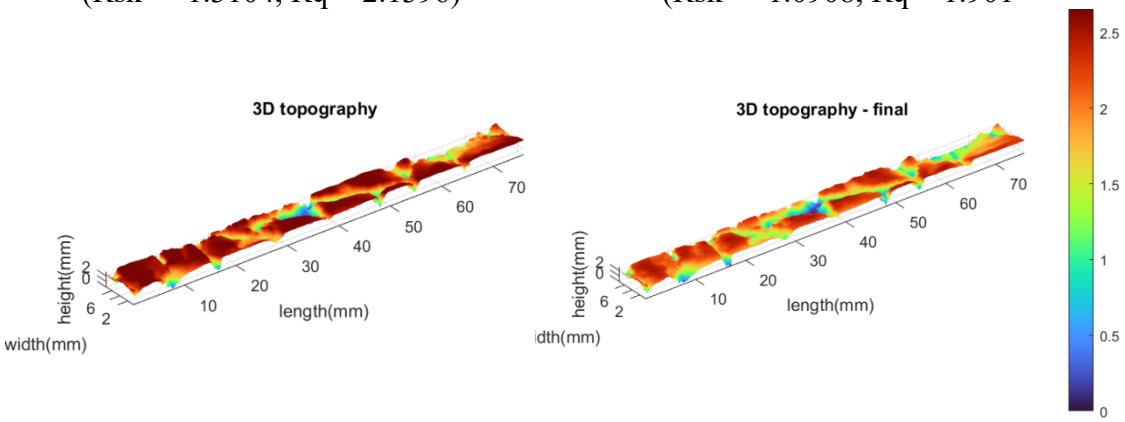

Granite

Final experimental texture
(Rsk = -1.1972, Rq = 1.8863)

Final model texture
(Rsk = -1.1349, Rq = 1.9111)

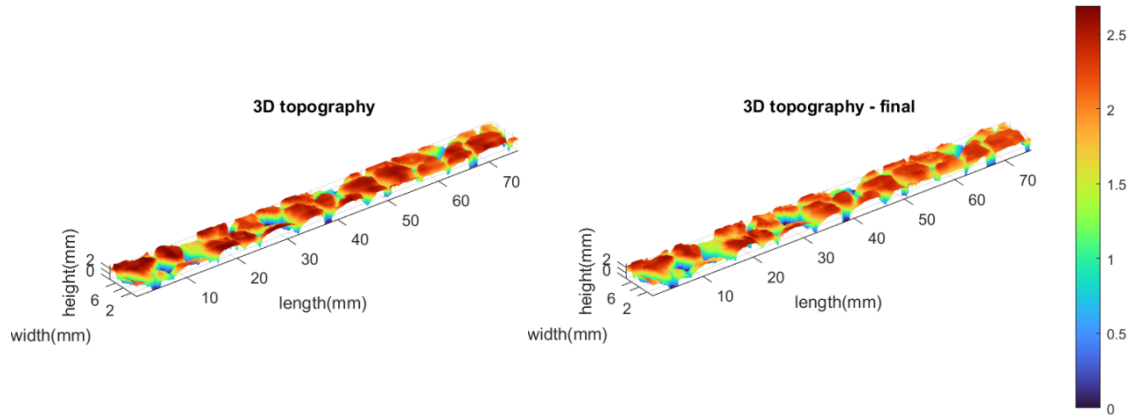

Figure 13: Comparison of the long-term mosaic pavement textures (Left: Experiment, Right: PSRM)

Conclusion

Here we proposed a new model to predict the evolution of skid resistance of pavements (PSRM) due to the polishing action of the traffic. PSRM combines both polishing and friction components. The polishing process combines a contact model and a wear law. A contact model considers the tire operating conditions, the tire tread material, the pavement texture, and the presence of water. The wear model within the PSRM considers the types of aggregates in the pavements and the resultant pressure distribution. The PSRM has been validated against experimental results. The "Wehner-Schulz" machine polished and successively measured the skid resistance of three different mosaic pavements comprised of different commonly used aggregates. The comparison between the experimental and simulated results showed strong agreement, although slight differences in their absolute values potentially highlight limitations in the wear law applied that did not consider the spatial distribution and the size of the minerals. Despite possible further improvements, the PSRM offers an exciting new and relatively complete prediction of skid resistance evolution that considers the traffic and the pavement conditions. This new predictive model has the potential to provide a new understanding of pavement deterioration and guide proactive mitigation and remediation of pavement networks, if the appropriate pavement composition is adequately known.

References

[1] Al-Mansour, A. I. (2006). Effects of Pavement Skid Resistance on Traffic Accidents. The Journal of Engineering Research [TJER], 3(1), 75–78. https://doi.org/10.24200/tjer.vol3iss1pp75-78

[2] M. KANE, K. SCHARNIGG (2009). Factors affecting parameters of tyre/road contact: skid resistance, noise emission and rolling resistance, Deliverable 10, TYROSAFE (Tyre and Road Surface Optimisation for Skid resistance and Further Effects), EU, PCRD, FP7/2007-2013, Juillet 2009

[3] UECKERMANN, Andreas, WANG, Dawei, OESER, Markus, et al. Calculation of skid resistance from texture measurements. Journal of traffic and transportation engineering (English edition), 2015, vol. 2, no 1, p. 3-16.

[4] Kane, M. A Contribution of the Analysis of the Road Macrotexture and Microtexture Roles vis-à-vis Skid Resistance, (2021) Journal of Testing and Evaluation 50 (ASTM International). https://doi.org/10.1520/JTE20210047

[5] YU, Miao, YOU, Zhanping, WU, Guoxiong, et al. Measurement and modeling of skid resistance of asphalt pavement: A review. Construction and building materials, 2020, vol. 260, p. 119878.

[6] CALLAI, Sergio Copetti Copetti et SANGIORGI, Cesare. A review on acoustic and skid resistance solutions for road pavements. Infrastructures, 2021, vol. 6, no 3, p. 41.

[7] TORBRUEGGE, Stefan et WIES, Burkhard. Characterization of pavement texture by means of height difference correlation and relation to wet skid resistance. Journal of traffic and transportation engineering (English edition), 2015, vol. 2, no 2, p. 59-67.

[8] KOKKALIS, A. G., TSOHOS, G. H., et PANAGOULI, O. K. Consideration of fractals potential in pavement skid resistance evaluation. Journal of Transportation Engineering, 2002, vol. 128, no 6, p. 591-595.

[9] Kane, M., Rado, Z., Timmons, A. Exploring the texture-friction relationship: From texture empirical decomposition to pavement friction. (2015) International Journal of Pavement Engineering, 16 (10), pp. 919-928. DOI: 10.1080/10298436.2014.972956

[10] - Rado, Z., Kane, M.An initial attempt to develop an empirical relation between texture and pavement friction using the HHT approach. (2014) Wear, 309 (1-2), pp. 233-246. DOI: 10.1016/j.wear.2013.11.015

[11] Kane, M., Edmondson, V., Long-term skid resistance of asphalt surfacings and aggregates' mineralogical composition: Generalisation to pavements made of different aggregate types, (2020) Wear, Volumes 454–455, 15 August 2020, 203339

[12] LEU, M. C. et HENRY, J. J. Prediction of skid resistance as a function of speed from pavement texture measurements. Transportation Research Record, 1978, vol. 666, p. 7-13.

[13] MILLER, Timothy, SWIERTZ, Daniel, TASHMAN, Laith, et al. Characterization of asphalt pavement surface texture. Transportation research record, 2012, vol. 2295, no 1, p. 19-26.

[14] SANDBERG, U. DEVELOPMENT OF AN INTERNATIONAL STANDARD FOR MEASUREMENT OF PAVEMENT MACROTEXTURE: ISO/DIS 13473-1. In : XXTH WORLD ROAD CONGRESS, MONTREAL, 3-9 SEPTEMBER 1995. INDIVIDUAL PAPERS PRESENTED UNDER THE AUSPICES OF THE COMMITTEES AND WORKING GROUPS. 1995.

[15] QIAN, Zhenyu et MENG, Lingjian. Study on micro-texture and skid resistance of aggregate during polishing. Frontiers of Structural and Civil Engineering, 2017, vol. 11, no 3, p. 346-352.

[16] WU, Xirong, ZHENG, Nanxiang, et KONG, Fansheng. The analysis of the factors affecting the macrotexture of bauxite clinker aggregate gradation. Construction and Building Materials, 2020, vol. 244, p. 118334.

[17] FLINTSCH, Gerardo W., DE LEÓN, Edgar, MCGHEE, Kevin K., et al. Pavement surface macrotexture measurement and applications. Transportation research record, 2003, vol. 1860, no 1, p. 168-177.

[18] BOND, R., KATEKKDA, I. E. D., LEES, G., et al. Tyre/Road Surface Interaction. Highway Engineer, 1976, vol. 23, no Analytic.

[19] VILLANI, M. M., ARTAMENDI, Ignacio, KANE, Malal, et al. Contribution of hysteresis component of tire rubber friction on stone surfaces. Transportation research record, 2011, vol. 2227, no 1, p. 153-162.

[20] Friel, S., Kane, M., Woodward, D., Use of wehner schulze to predict skid resistance of Irish surfacing materials, (2013) Airfield and Highway Pavement 2013: Sustainable and Efficient Pavements - Proceedings of the 2013 Airfield and Highway Pavement Conference, pp. 817-828.

[21] KANE, Malal et EDMONDSON, Vikki. Modelling the bitumen scour effect: Enhancement of a dynamic friction model to predict the skid resistance of rubber upon asphalt pavement surfaces subjected to wear by traffic polishing. Wear, 2018, vol. 400, p. 100-110.

[22] Do, M.-T., Tang, Z., Kane, M., de Larrard, F., Evolution of road-surface skid-resistance and texture due to polishing, (2009) Wear, 266 (5-6), pp. 574-577.

[23] Kane, M., Artamendi, I., Scarpas, T., Long-term skid resistance of asphalt surfacings: Correlation between Wehner-Schulze friction values and the mineralogical composition of the aggregates, (2013) Wear, 303 (1-2), pp. 235-243.

[24] Kane, M., Zhao, D., De-Larrard, F., Do, M.-T., Laboratory evaluation of aggregate polishing as a function of load and velocity. Application to the prediction, of damages on skid resistance of road surfaces due to trucks and passenger cars, (2012) Road Materials and Pavement Design, 13 (2), pp. 312-326.

[25] KANE, Malal et EDMONDSON, Vikki. Long-term skid resistance of asphalt surfacings and aggregates' mineralogical composition: Generalisation to pavements made of different aggregate types. Wear, 2020, vol. 454, p. 203339.

[26] TOURENQ C., FOURMAINTRAUX D., Propriétés des granulats et glissance routière, Bulletin de liaison des Laboratoires des Ponts et Chaussées, 51, 1971, pp. 61 à 69.

[27] KANE, Malal, DO, Minh Tan, et PIAU, Jean Michel. On the study of polishing of road surface under traffic load. Journal of transportation engineering, 2010, vol. 136, no 1, p. 45-51.

[28] Kane, M., A contribution to tire/road friction modeling: From a simplified dynamic frictional contact model to a "Dynamic Friction Tester" model, (2015) Wear, 342-343, pp. 163-171.

[29] KANE, Malal, DO, Minh-Tan, CEREZO, Veronique, et al. Contribution to pavement friction modelling: an introduction of the wetting effect. International Journal of Pavement Engineering, 2019, vol. 20, no 8, p. 965-976.

[30] KANE, Malal et EDMONDSON, Vikki. Tire/road friction prediction: Introduction a simplified numerical tool based on contact modelling. Vehicle System Dynamics, 2020, p. 1-20.

[31] KANE, Malal et EDMONDSON, Vikki. Aggregates mineralogical composition dataset to estimate the averaged aggregate hardness parameter to predict the long-term skid resistance of pavements. Data in Brief, 2020, vol. 31, p. 105849.

XXX.